IAEA
International Atomic Energy Agency

22nd IAEA Fusion Energy Conference

Geneva, Switzerland 13-18 October 2008

ELM power loadings and control on MAST using resonant magnetic perturbations

A. Kirk, E. Nardon, B. Ayed, G. Cunningham, S. Lisgo, H. Meyer and the MAST team

EURATOM/UKAEA Fusion Association, Culham Science Centre, Abingdon, Oxon OX14 3DB, UK

ELM power loadings and control on MAST using resonant magnetic perturbations

A. Kirk, E. Nardon, B. Ayed, G. Cunningham, S. Lisgo, H. Meyer and the MAST team

EURATOM/UKAEA Fusion Association, Culham Science Centre, Abingdon, Oxon OX14 3DB, UK

e-mail contact of main author: andrew.kirk@ukaea.org.uk

Abstract. A study of the evolution of the filaments observed during Type I ELMs on MAST is presented. The ion saturation current e-folding length of the filaments shows a weak, if any, dependence on the size of the ELM ($\Delta W_{ELM}/W_{ped}$). The measured radial velocities of the filaments also show at most a weak dependence on $\Delta W_{ELM}/W_{ped}$. A model, based on the observed evolution of the filaments, has been developed, that is in reasonable agreement with the observed ELM energy losses and target profiles. This model has been used to predict the target and first wall loads in ITER. Experiments have been performed using both internal and external resonance magnetic perturbation coils and initial results are presented.

1. Introduction

In existing devices type-I ELMs result in the sudden release of 5-15 % of the pedestal stored energy in a short amount of time (100-300μs). If this behaviour extrapolates to future devices, such as ITER, type I ELMs may lead to unacceptably high-energy loads to the divertor plates and plasma facing components [1]. However, there is considerable uncertainty associated with such predictions because of a lack of understanding of the processes involved. In this paper, the evolution, radial extent and spatial structure of type-I ELMs on MAST will be presented. Using these observations a model has been constructed that can describe the spatial distribution of ELM energy at the divertor targets in MAST and predict the distributions for ITER. All current models, this one included, indicate that in order to ensure an adequate lifetime of the divertor targets on ITER a mechanism to decrease the amount of energy released by an ELM, or to eliminate ELMs altogether is required. One such amelioration mechanism relies on perturbing the magnetic field in the edge plasma region. MAST is equipped with both external and internal coils and preliminary experiments using these coils are presented in section 4.

2. ELM evolution on MAST

Although it is clear that filament structures exist during ELMs (see [2] and reference therein) it is still uncertain what parameters determine how much energy these filaments transport to the wall and what determines their size and how they propagate. This is mainly due to the lack of experimental data. In order to increase the data available, experiments have been performed on MAST measuring, as a function of ELM size, both the radial expansion of individual filaments and the mid-plane radial e-folding length of particles and energy. In the simplest picture, where the filaments propagate out radially with a constant velocity (V_r) and lose particles on ion parallel transport timescales ($\tau_{//} = L_{//}/c_s$, $L_{//}$ is the connection length and c_s the ion sound speed), then the particle e-folding length (λ) can be expressed as $\lambda \sim V_r \tau_{//} \sim V_r L_{//}/c_s$. In this paper measurements of the ion saturation current (I_{SAT}) as a function of

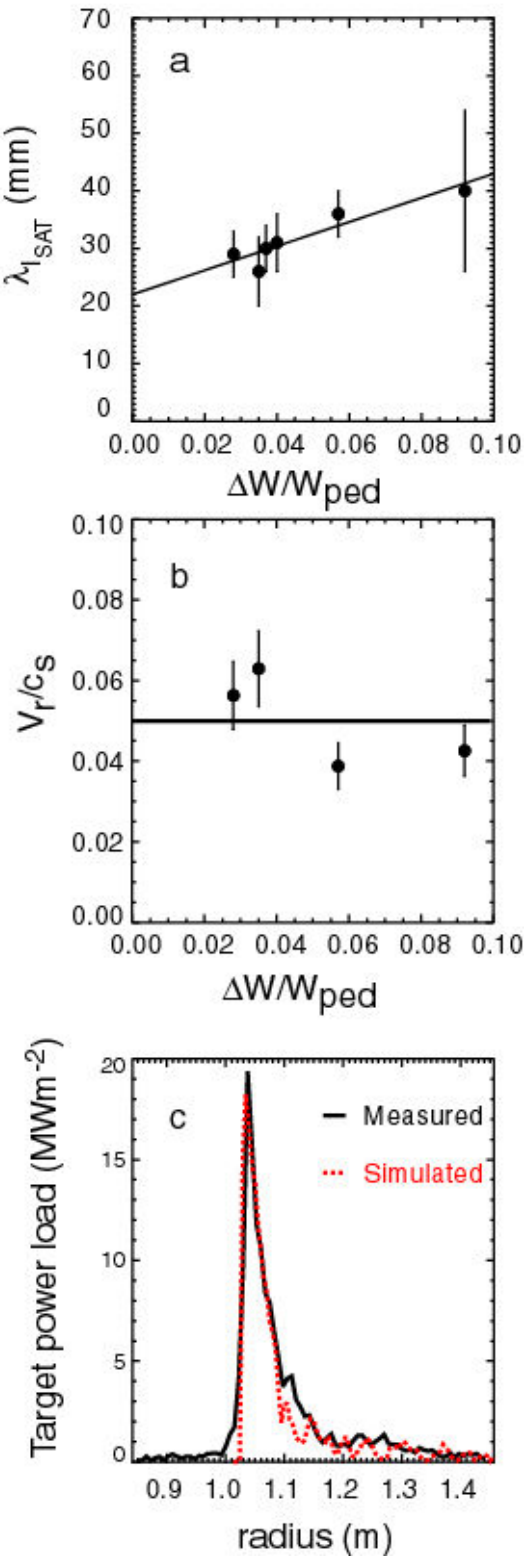

Figure 1 a) λ_{ISAT} as a function of a) $\Delta W/W_{ped}$, b) the radial velocity of the filaments as a fraction of the sound speed as a function of $\Delta W/W_{ped}$ and c) the measured and simulated divertor target radial power profile.

radial distance have been fitted with an exponential in order to determine the e-folding length (λ_{ISAT}), which is assumed to represent the power e-folding length of the radial efflux [3]. Scans have been performed over plasma parameters including ELM size and pedestal temperature produced by changing the pedestal density (in the range $1.5 < n_e^{ped} < 6x1019$ m^{-3}) and/or the injected beam power (in the range $1.5 < P_{NBI} < 3.8$ MW). Figure 1a shows a plot of λ_{ISAT} on MAST Upgrade as a function of the fraction of the pedestal energy released by an ELM ($\Delta W_{ELM}/W_{ped}$). Although any dependence of the e-folding length is small compared to the scatter in the underlying data, a small increase in the e-folding length with $\Delta W_{ELM}/W_{ped}$ cannot be excluded.

The data, have been fitted to the form $\lambda = \lambda_{fil} + \alpha(\Delta W/W_{ped})$ which yields λ_{fil} = 23 ±3 mm (MAST), where λ_{fil} represents the initial radial distribution of energy within the filament i.e. what would be measured if a probe was reciprocated into the filament while it was still attached to the plasma and not moving radially.

Note the higher $\Delta W_{ELM}/W_{ped}$ discharges in figure 1a have a higher T_e^{ped}. At higher temperatures the filament density should decrease more quickly due to parallel transport. This should then reduce the e-folding length, which is not observed. One explanation might be that the velocity (acceleration) of the filaments increases with T_e^{ped}. In order to investigate this further the velocity of the filaments has been measured directly by tracking the evolution of the filaments observed in visible images for shots with different $\Delta W_{ELM}/W_{ped}$ and T_e^{ped}. As was reported in [4], although not all the filaments within a given ELM have the same size, the mean and standard deviation of the distribution of sizes does not change with $\Delta W_{ELM}/W_{ped}$ i.e. on average there is no evidence that larger ELMs have larger filaments. The radial location of each filament during an ELM has been found as a function of time. For each value of $\Delta W_{ELM}/W_{ped}$ the filaments in several ELMs have been tracked and the radial location (Δr_{LCFS}) of each filament as a function of time has been determined. On average the filaments in ELMs with high $\Delta W_{ELM}/W_{ped}$ expand away from the LCFS faster than the ones at low $\Delta W_{ELM}/W_{ped}$. Although the accelerating hypothesis

best describes the underlying radial profiles, figure 1b plots the results of the fits assuming a constant velocity (as a function of radius) as a fraction of the ion sound speed versus $\Delta W_{ELM}/W_{ped}$. The general conclusion is that there is little evidence that the radial velocity as a function of the ion sound speed depends strongly on $\Delta W_{ELM}/W_{ped}$. However, this does imply that the radial velocities increases as $\sqrt{T}$.

3. Modelling the structure of ELMs and implications for ITER

Based on the observations of the evolutions of the filaments during ELMs the most probable ELM energy loss process is as follows: for the first 50-100 μs, filaments remain near to the LCFS. During this time the filaments enhance losses from the core and the radial distribution of these losses has an e-folding length that is determined by the radial size of the filament. After this time the filaments move radially away from the LCFS with each filament containing up to 2.5 % of ΔN_{ELM} and ΔW_{ELM}. The particles and energy in the filaments is subsequently lost by parallel transport along open field lines to the targets. This representation of the ELM event has been incorporated into a Monte Carlo code in order to simulate the target power profiles assuming that the process is dominated by ion parallel transport. On MAST, the first wall/limiter is a long way from the plasma and hence effectively all the energy released by an ELM arrives at the target. Figure 1c shows the simulated and observed divertor target radial power profiles normalised such that the peak agrees with the peak measured experimentally. The model describes not only the amount of power arriving in the remote part of the target but also the near separatrix profile.

A simulation has also been used to predict the target profiles in the ITER H-mode baseline scenario [6], which starts off with 12 filaments each parameterised to have Gaussian density and energy profiles with σ_r = 1.6 cm and $\sigma_\perp$ = 5 cm (the size of the filaments in the radial direction (σ_r) and perpendicular to both the field line and the radial direction ($\sigma_\perp$)), based on the extrapolations obtained in [5]. The initial ion temperature in the filament is assumed to be half of the pedestal top i.e. 1.5 keV. For a period of 50 μs half of the filament protrudes from the LCFS and the filaments rotate with the pedestal velocity and release particles into the SOL. After this time individual filaments decelerate toroidally and move away radially, each carrying up to 2.5 % of the total number of particles lost. In both the connected and separated stage the particles are traced along the local field line to the divertor target. Determining the radial velocity of the filaments on current devices is difficult and relies on several assumptions, which makes extrapolations prone to error. To demonstrate the sensitivity of the results to the radial velocity used, two simulations have been performed using V_r= 0.5 and 1 kms^{-1}.

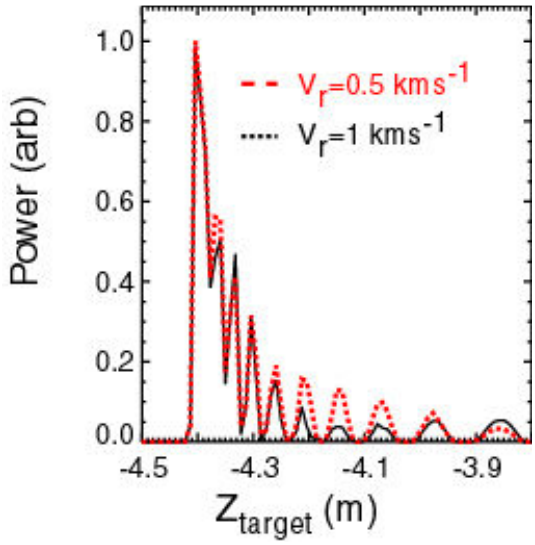

Figure 2 The predicted target distributions on ITER at a given toroidal location.

The resulting mid-plane density and ion temperature profiles show that typically between 15 and 40 % of the initial particle content of the filaments reaches the wall with ion temperatures in the range of 200 to 500 eV. The profiles have been fitted with an exponential in the region 0.02 $<\Delta r_{LCFS}<$0.06 m, (where Δ_{rlCFS} is the radial distance from the LCFS) and yield e-folding lengths of λ_{ne} = 2.8 (5.6) cm and λ_{Ti} = 3.6 (5.7)

cm for V_r= 0.5 kms^{-1} (V_r = 1kms^{-1}). These values are similar to those found using a fluid based model where the parallel losses are treated with diffusive and advective removal times [7].

The simulation can also be used to predict the divertor target profile and the fraction of power arriving at the limiter, which is located 6 cm from the LCFS at the mid-plane and in the tail of the target profile. The resulting target profiles at a particular toroidal location are shown in figure 2, where significant structure can be observed in the remote region of the target. In order to calculate the amount of energy arriving at the limiter a 2-D profile of the ITER limiter has been incorporated into the model. If a particle in the filament intercepts the limiter before arriving at the target its energy is assumed to have been deposited at the limiter. The fraction of the ELM energy deposited on the limiter is 4.0 (15.5) % for V_r= 0.5 kms^{-1} (V_r = 1kms^{-1}). The fraction of energy arriving in the tail of the target profile, defined as Z > -4.2 m, is 17.7 (10.9) %.

4. ELM Mitigation experiments

All current models, this one included, indicate that in order to ensure the lifetime of the divertor targets on ITER a mechanism to decrease the amount of energy released by an ELM, or to eliminate ELMs altogether is required. One such amelioration mechanism relies on perturbing the magnetic field in the edge plasma region, enhancing the transport of particles and keeping the edge pressure gradient below the critical value that would trigger an ELM. This technique has been successfully employed on DIII-D using two up-down symmetric sets of 6 in-vessel coils [8] and more recently on JET using the external error field correction coils [9]. MAST is equipped with both a set of ex-vessel error field correction coils (EFCCs), similar to JET, and more recently with a set of 12 in-vessel coils, similar to those used in DIII-D.

4.1 Experiments using the external coils

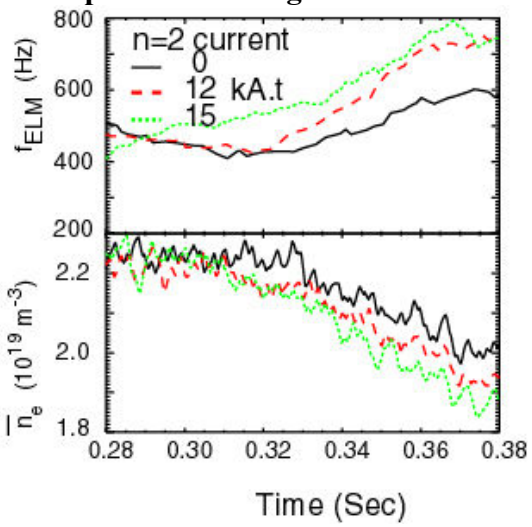

Figure 3: The effect of applying an n=2 error field to a series of discharges with low pedestal collisionality (ν_e^*=0.3).

ELM mitigation experiments have been performed using n=1 and n=2 fields from the ex-vessel coils. With an n=1 configuration of the coils a delay in the L-H transition was observed with increasing error field. Further n=1 experiments were performed by delaying the application of the field until after the L-H transition, however, it was difficult to find an operational window where sufficient current could be applied without either causing a back transition H-L or locked mode. This is somewhat similar to the behaviour seen on JET, where a narrow window depending on edge q was found between ELM mitigation and locked mode onset.

Experiments were also performed using an n=2 configuration, where 2 of the four error field coils were re-wired in parallel to produce a dominantly n=2 harmonic perturbation and the remaining 2 coils were left wired in an anti-parallel configuration to cancel the n=1 component of the intrinsic error field.

Figure 3 shows the results obtained by applying a n=2 perturbation in a series of low pedestal collisionality (ν_e^*=0.3) discharges (reference discharge: #18740, double null plasma with 3.2 MW of neutral beam heating, plasma current I_p=750 kA and toroidal magnetic field on the magnetic axis [R_{mag}=0.92m] B_t=-0.52T), using EFCCs currents of I_{EFCC}=0 (for

reference), 12, and 15kAt. Notice that the ELMs in this type of discharge have a high natural frequency (~500Hz) and cannot be classified as Type I ELMs. Nevertheless, the EFCCs were observed to increase their frequency by typically 50 %. The evolution of the line integrated density shows that the EFCCs enhance the rate of density drop (without EFCCs, these plasmas have a naturally decreasing density). This is reminiscent of the density pump-out observed in experiments on DIII-D [8] and JET [9].

Calculations of the perturbation to the plasma for 15 kA.t in the coils has been performed using the ERGOS code (vacuum magnetic modelling) [10]. The ergodised layer is defined as the region for which the Chirikov parameter (σ_{ch}) is greater than 1 [10]. The σ_{Ch} profile for the case with I_{EFCC}=15kAt is presented in Fig. 4 together with profiles from shots on DIII-D and JET in which ELM mitigation has been observed [11]. The MAST profile is clearly above the DIII-D and JET profiles. This is due to the large magnetic shear at the edge of MAST, which supports the overlapping of islands. From the edge ergodisation criterion, a suppression of the Type I ELMs could therefore be expected. The fact that ELM suppression is not observed here could be due to the fact that these ELMs are not Type I ELMs, but also to the insufficiency of the vacuum modelling, or to the fact that edge ergodisation by itself is not sufficient for ELM suppression. It is interesting to note that, to date, complete suppression has not been observed on any device using a single row of mid-plane coils.

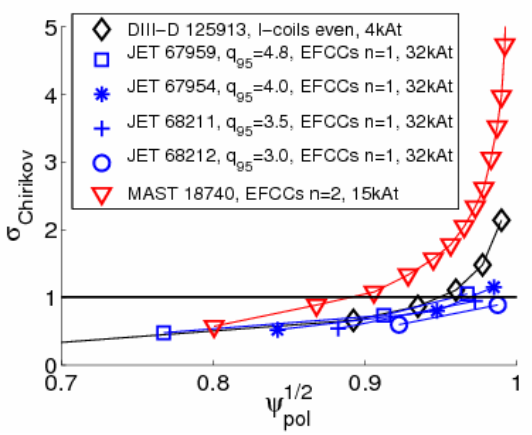

Figure 4 Calculated Chirikov parameter profiles for DIII-D, JET and MAST.

4.2 Experiments using the internal coils

Figure 5 Montage of 6 photographs at different toroidal locations showing the 12 installed ELM mitigation coils. The upper and lower ELM coils are indicated in the 4th image.

The difference between on and off-axis coils will be investigated further following the installation on MAST in December 2007 of a set of 12 in-vessel coils (6 upper and 6 lower), similar in layout to those used in DIII-D, see Figure 5. The coils are constructed from an aluminium alloy and are composed of 4 turns each. The coils measure 270 by 600 mm and are designed to carry currents up to 2 kA, although the current power supplies are limited to 1.4 kA. To electrically insulate the coils they are coated in aluminium oxide and are then encased inside a boron nitride shell, which is then coated in colloidal graphite. The coils can be operated in either "even" (where the current in the upper and lower coil at the same toroidal location has the same sign) or "odd" (the current in the upper and lower coil have opposite sign) parity mode.

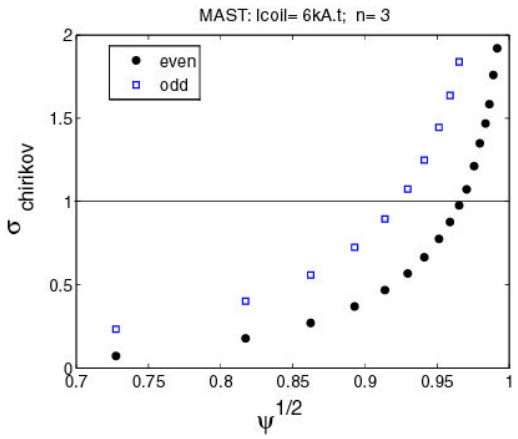

Figure 6 Calculated Chirikov parameter profiles for MAST internal coils in even and odd parity.

Profiles of σ_{Ch} calculated using the ERGOS code for a typical MAST equilibrium and for a current of 6kAt, are shown in Figure 6. Due to the large pitch angle on the Low Field Side (LFS) on MAST, the poloidal mode spectrum of the applied field is different (more stretched in m) compared with DIII-D. Hence, for typical MAST equilibria, which have $q_{95} < 6$, the odd parity configuration is predicted to produce the largest effect. The coils can produce $\sigma_{Ch}>1$ for $\psi_{pol}^{1/2} > 0.91$, which is slightly better than the MAST EFCCs in an n=2 configuration, and clearly better than the I-coils on DIII-D or the EFCCs on JET.

Preliminary commissioning experiments performed in low current (400 kA) Ohmic plasmas. The q_{95} in these plasmas is higher (6-8) than that in normal H-mode plasmas and as such the applied perturbation is resonant in the even configuration (see Figure 7). The Chirikov parameter profile shows that the ergodised region is much broader in the case of the even parity configuration.

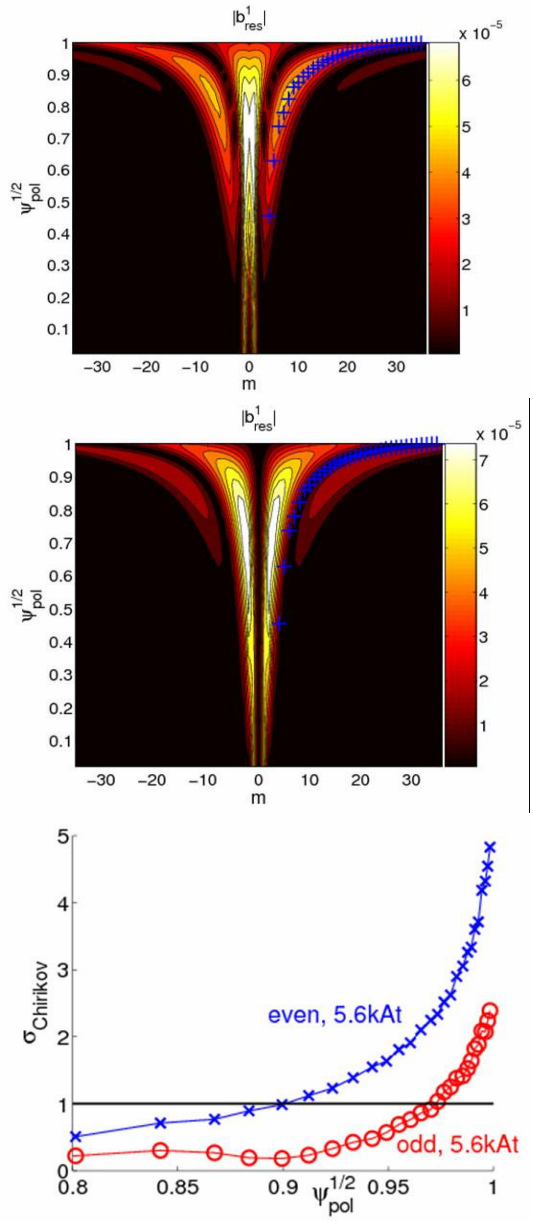

Figure 7 Poloidal magnetic spectrum for the n=3 even and odd parity configurations. Superimposed as the blue crosses are the q=m/3 rational surfaces. The calculated Chirikov parameter profiles for both cases.

The commissioning experiments showed that the coils and power supplies could be reliably operated and no problems were observed during disruptions. Experiments were performed using different coil configurations (both odd and even and with the perturbation rotated by 60°) and different coil currents. In the odd parity configuration no effect was observed on the plasma. In the even parity configuration a clear and repeatable effect was observed on the density in the time period 150 – 400 ms (see figure 8). The density first decreased in the time period 150-300 ms and then increased in the region 300-400 ms. The gas puff rate was held constant in these shots and there was no active pumping.

4. Summary

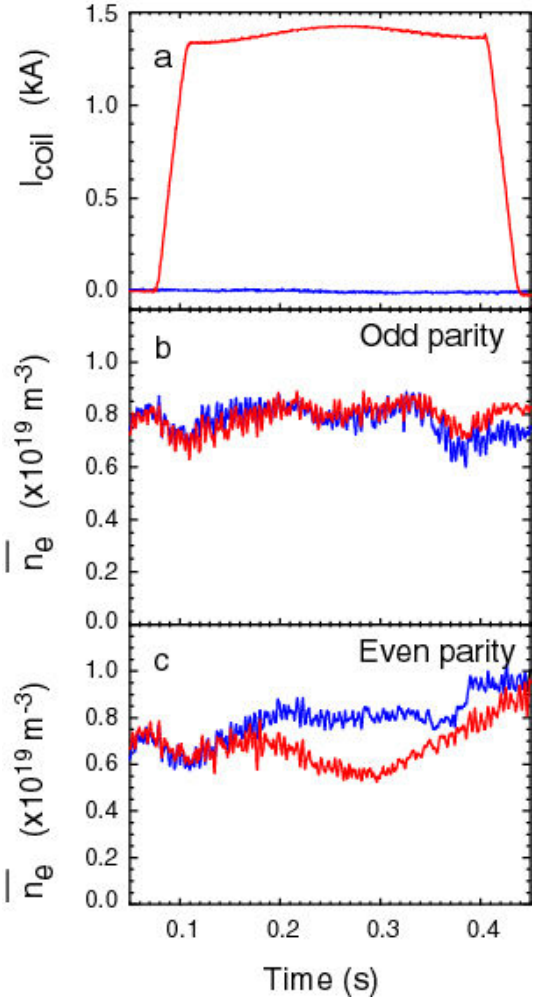

Figure 8 Ohmic experiments using the internal coils in Odd and Even parity mode. a) the applied coil current. The line average density in b) Odd and c) Even parity mode shots with 0 (blue) and 1.4 kA (red) current in the coils.

In this paper results from MAST on the effect of ELM size on the propagation of filaments observed during type I ELMs have been presented. The ion saturation current e-folding length of the filaments shows a weak, if any, dependence on the size of the ELM ($\Delta W_{ELM} / W_{ped}$). The measured radial velocities of the filaments also show at most a weak dependence on $\Delta W_{ELM} / W_{ped}$. The results from a simple model based on parallel transport have been presented, which can explain the target power profile and the amount of power arriving at the remote parts of the target. This model has two unknown input parameters: the initial ion temperature in the filament (T_i) and the radial velocity (V_r). Simulations have been presented for ITER based on the H-mode baseline scenario. These simulations assumed that the ion temperature was half that of the pedestal and two possible value of V_r have been used. The results presented show that between 4 and 15 % of the ELM energy may be deposited on the limiters.

MAST is equipped with both internal and external resonant magnetic perturbations coils. Vacuum modelling with ERGOS shows that the Chirikov parameter is greater in MAST than in DIII-D and JET. Hence if edge ergodisation is the mechanism responsible for ELM mitigation then it should be reproducible on MAST. Results obtained with the external coils in an n=2 configuration do show an effect on the ELMs. Commissioning of new internal coils dedicated to ELM control is ongoing. Preliminary results in Ohmic plasmas show an effect on the density when the coils are in the even parity configuration, which is predicted to be optimum from the ERGOS modelling.

Acknowledgements

UKAEA authors were funded jointly by the United Kingdom Engineering and Physical Sciences Research Council and by the European Communities under the contract of Association between EURATOM and UKAEA. The views and opinions expressed herein do not necessarily reflect those of the European Commission.

References

[1] Loarte A *et al.* 2002 *Plasma Phys. Control. Fusion* **44** 1815

[2] Kirk A *et al*. 2005 *Plasma Phys. Control. Fusion* **47** 995
[3] Herrmann A *et al.* 2007 *J. Nucl. Mater.* **363-365** 528
[4] Kirk A *et al*. 2007 *Plasma Phys. Control. Fusion* **49** 1259
[5] Kirk A et al. 2008 *J. Phys.: Conf. Ser*. **123** 012011
[6] Polevoi A *et al*., 2002 J. Plasma Fusion Res. **5** 82
[7] Fundamenski W and Pitts R A 2007 *J. Nucl. Mater.* **363-365** 319
[8] Evans T *et al*., 2004 *Phys. Rev. Lett.* **92** 235003
[9] Liang Y. *et al.*, 2007 *Phys. Rev. Lett.* **98** 265004
[10] Nardon E. *et al*., 2007 *J. Nucl. Mater.* **363-365** 1071
[11] Nardon E. *et al*., 2008 "ELM control by resonant magnetic perturbations on JET and MAST", Submitted to *J. Nucl. Mater.*